Primary renal parenchymal squamous cell carcinoma: a case report and literature review

Lingze Hu[1], Dilare Aximu[1], Qianqian Yang[2], Liejun Mei[1]*, Fenfang Zhou[1]*

[1]Department of Medical Imaging, Zhongnan Hospital of Wuhan University, China
[2]Department of Pathology, Zhongnan Hospital of Wuhan University, China

Submitted: 21 February 2026; **Accepted:** 30 August 2026
Online publication: 31 August 2026

Arch Med Sci
DOI: https://doi.org/10.5114/aoms/235877

***Corresponding authors:**
Liejun Mei,
Fenfang Zhou
Department of Medical Imaging
Zhongnan Hospital
of Wuhan University
Wuhan, China
E-mail: meilj1971@163.com,
zhoufenfang@whu.edu.cn

Renal squamous cell carcinoma (SCC) is classified into parenchymal and pelvic types, with the pelvic type being more common. Primary renal parenchymal SCC accounts for only 0.5–0.8% of all renal malignancies [1], and is exceedingly rare, with only 26 previously reported cases documented in the literature to date. Owing to its non-specific clinical and imaging features, primary renal parenchymal SCC is often diagnosed at an advanced stage, usually presenting as a renal parenchymal mass.

Herein, we report an unusual case of histopathologically confirmed primary renal parenchymal SCC that presented with left flank pain and an absence of typical urinary symptoms such as gross hematuria, urinary frequency, urgency, or dysuria. Imaging showed a mass in the upper pole of the left kidney, accompanied by a filling defect within the left renal vein. The patient underwent laparoscopic unilateral nephrectomy, and subsequent histopathological examination demonstrated carcinoma invasion into the renal sinus fat, local extension to the renal pelvic urothelium, and involvement of the perihilar perivascular adipose tissue. We present the imaging and pathological findings of this case and review the relevant literature to provide clinical context for the diagnosis and management of primary renal parenchymal SCC.

A 76-year-old female patient presented to local hospital with left flank distending pain for over one month, which had worsened over the past 3 days. The pain began without an obvious cause and was not accompanied by gross hematuria, urinary frequency, urgency, or any other urinary symptoms. Physical examination upon admission revealed a soft abdomen without tenderness, rebound tenderness, or muscle guarding. Palpation of the renal regions did not elicit tenderness, and there were no signs of lower extremity edema or other abnormal physical findings. Dry chemistry urinalysis and quantitative urine sediment analysis revealed a positive occult blood test result (++) with an erythrocyte count of 50.10/µl. Microscopic examination of the urine smear showed no high-grade urothelial carcinoma cells; only a few well-differentiated urothelial cells and squamous epithelial cells were observed.

Renal–ureter–bladder color Doppler ultrasonography showed a hypoechoic mass measuring approximately 6.4 × 4.2 cm at the upper pole of the left kidney. The mass had ill-defined margins, projected outward, and showed little blood flow. The initial diagnosis was a left renal space-occupying lesion. Computed tomography (CT) revealed an irregular, slightly hyperdense mass measuring approximately 60 × 48 × 56 mm in the mid-upper segment of the left kidney, with heterogeneous internal

density and an indistinct boundary from the normal renal parenchyma (Figure 1 A). After contrast injection, the mass showed marked heterogeneous enhancement with small internal nodular areas lacking enhancement. Additionally, a filling defect in the left renal vein was detected, along with significant thickening of the perirenal fascia and mild inflammatory exudation (Figures 1 B–E). Multiple enlarged retroperitoneal lymph nodes were also seen. CT urography (CTU) revealed heterogeneous and diminished contrast opacification in the left kidney compared with the contralateral side (Figure 1 F). Magnetic resonance imaging (MRI) showed an irregular lesion in the left renal parenchyma. The lesion was isointense on T1-weighted images and slightly hyperintense on T2-weighted images, with an indistinct boundary from the adjacent renal parenchyma and renal sinus (Figures 1 G–N). On diffusion-weighted imaging (DWI), the lesion showed restricted diffusion signals and mildly decreased apparent diffusion coefficient (ADC) values; some cystic components contained nodular areas with markedly restricted diffusion (Figures 1 O and 1 P). After contrast administration, the lesion was heterogeneously enhanced. The left renal pelvis was poorly visualized. The proximal left renal vein showed heterogeneous signal intensity, accompanied by mild linear perirenal exudative changes. Several lymph nodes were seen in the left renal hilar region and retroperitoneum.

The patient underwent a laparoscopic unilateral nephrectomy. Intraoperatively, the upper pole of the left kidney showed significant enlargement and induration.

Gross pathological examination revealed that the resected left kidney measured 9.5 × 5.5 × 4 cm. Multiple sections were made along the maximum surface. A grayish-yellow mass measuring 6.3 × 5.1 × 3.9 cm was predominantly located in the renal parenchyma of the upper pole, with focal extension into the renal pelvis. It appeared to invade the renal sinus fat and perihilar perivascular adipose tissue but did not extend beyond the renal capsule. Microscopically, the tumor grew infiltratively in nested and sheet-like patterns. Small foci of necrosis were present (Figure 2 A). Focal gland-forming areas were identified, with necrotic material within the lumina (Figure 2 B). The intervening stroma showed areas of fibrosis and lymphocytic infiltration. Tumor cells had indistinct borders and eosinophilic cytoplasm, with eosinophilic material in the cytoplasm. Marked cytologic atypia was present, with enlarged hyperchromatic nuclei, prominent pleomorphism, and atypical mitotic figures (Figure 2 C). The tumor invaded the renal sinus adipose tissue and locally involved the renal pelvic urothelium. In addition, carcinoma infiltration was identified in the perihilar perivascular adipose tissue. The remaining renal parenchyma showed prominent chronic inflammatory cell infiltration with lymphoid follicle formation (Figure 2 D).

The tumor exhibited markedly malignant histopathological characteristics. The nest-like distribution of tumor cells, eosinophilic cytoplasm, intracellular red-stained substances, and the presence of background lymphocytes suggested squamous differentiation. The main differential diagnosis was urothelial carcinoma with squamous differentiation. Furthermore, considering the tumor's anatomical location and morphological features, additional differential diagnoses included clear cell renal cell carcinoma, chromophobe renal cell carcinoma, collecting duct carcinoma, and other renal neoplasms characterized by distinct molecular alterations. The tumor's high-grade histological features and positive expression of PAX8, CAIX, CK, and CK7, together with a Ki-67 index of approximately 70%, supported the diagnosis of a high-grade malignant epithelial tumor. GATA3 positivity was observed but was not interpreted as evidence of squamous differentiation. The most common malignant tumor of the renal parenchyma is clear cell renal cell carcinoma. In some high-grade cases, the cytoplasm can also be eosinophilic, rich in glycogen and lipids. However, clear cell renal cell carcinoma typically exhibits a rich network of thin-walled vessels, lacks squamous differentiation, and is generally negative for CK7. These findings argued against this diagnosis. Similarly, the absence of characteristic features such as well-defined plant cell-like membranes, perinuclear halos, and CD117 expression argued against chromophobe renal cell carcinoma. Additionally, the lack of tubular structures and hobnail cells, together with the large tumor cells and inconspicuous fibrous stroma, further excluded collecting duct carcinoma. Moreover, preserved SDHB and FH expression on immunohistochemistry argued against renal tumors associated with loss of either protein. Eosinophilic cytoplasm and stromal inflammatory infiltration provided additional morphologic support. The squamous phenotype was supported primarily by the tumor morphology and concordant expression of CK5/6, P40, and P63 in the squamous areas. In areas with focal glandular differentiation, GATA3 remained positive, whereas P40, P63, and CK20 were negative. Because typical morphologic features of urothelial carcinoma were not identified microscopically, urothelial carcinoma with squamous differentiation was considered unlikely. Furthermore, the patient had no history of primary tumors at other sites, including the head and neck or lungs, making metastatic squamous cell carcinoma unlikely. Overall, the

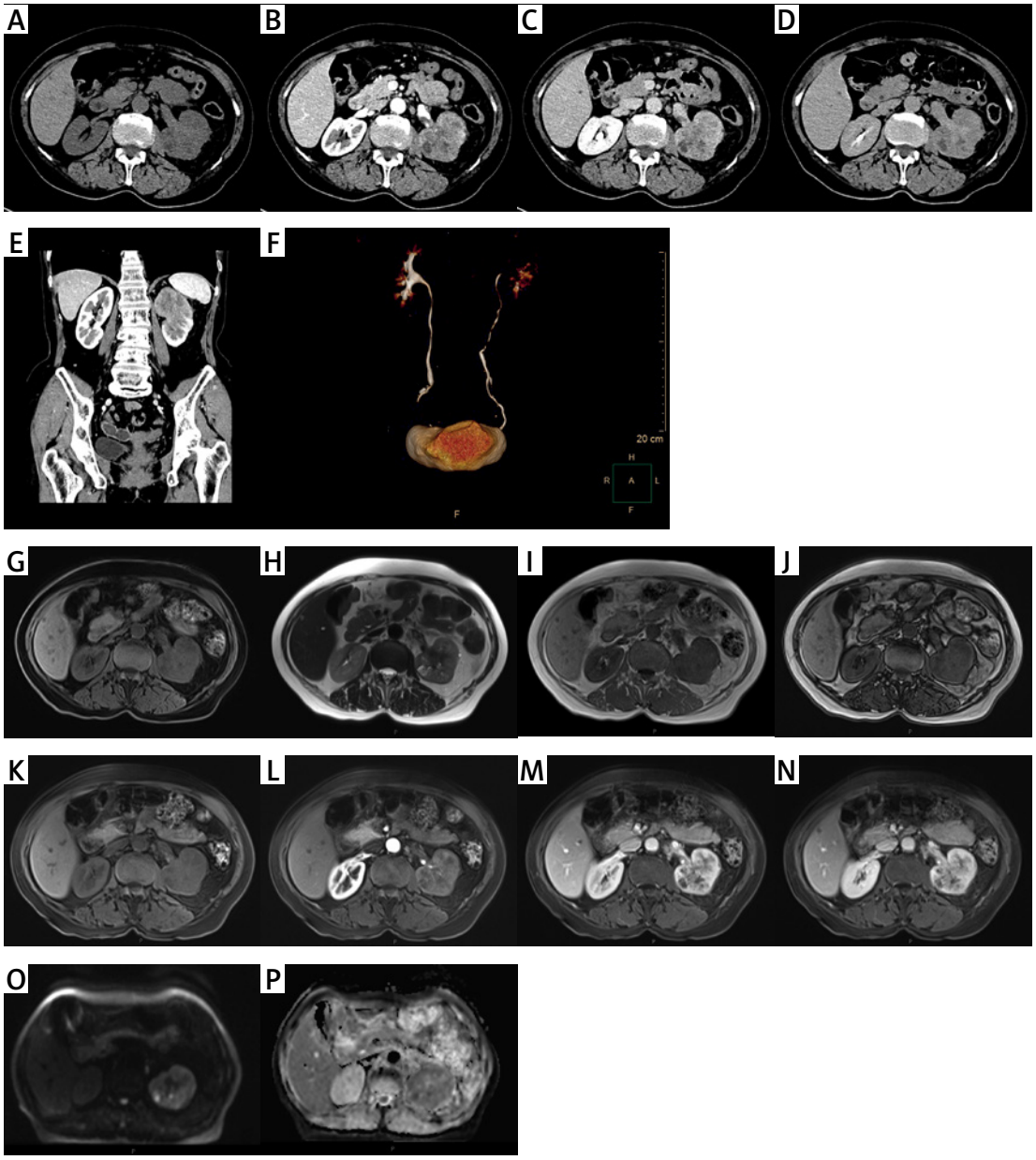

Figure 1. Representative computed tomography (CT), computed tomography urography (CTU) and magnetic resonance imaging (MRI) images of the patient: **A** – Non-contrast abdominal CT scan axial image shows an irregular, slightly hyperdense mass in the left mid-to-upper kidney, with heterogeneous density. **B** – Artery phase, contrast-enhanced scan shows marked heterogeneous enhancement with small nodular non-enhancing foci. **C** – Venous phase, the left renal vein shows a suspected filling defect. **D** – Excretory phase shows no abnormal density in the bilateral ureteral courses. **E** – Coronal view shows a slightly hyperdense mass with heterogeneous density in the upper pole of the left kidney, with parenchymal invasion and ill-defined margins. **F** – CTU shows contrast opacification in bilateral pelvises, calyces, and ureters. The left kidney demonstrates heterogeneous, reduced contrast filling compared to the right. The ureter is fully visualized without significant dilation or stricture. **G** – Axial T1-weighted non-contrast image shows an irregular lesion in the left renal parenchyma with isointense signal. **H** – Axial T2-weighted non-contrast image shows the lesion with slightly hyperintense signal. **I** – Axial T1-weighted in-phase image. **J** – Axial T1-weighted opposed-phase image. **K** – Axial T1-weighted pre-contrast mask image. **L** – Axial T1-weighted arterial phase image shows low signal intensity in the left kidney and indistinct renal pelvis. **M** – Axial T1-weighted venous phase image shows heterogeneous signal in the proximal renal vein. **N** – Axial T1-weighted excretory phase image. **O** – Diffusion-weighted imaging (DWI) shows restricted diffusion, with nodular markedly hyperintense signals in some cystic components. **P** – The corresponding apparent diffusion coefficient (ADC) map shows slightly decreased ADC value

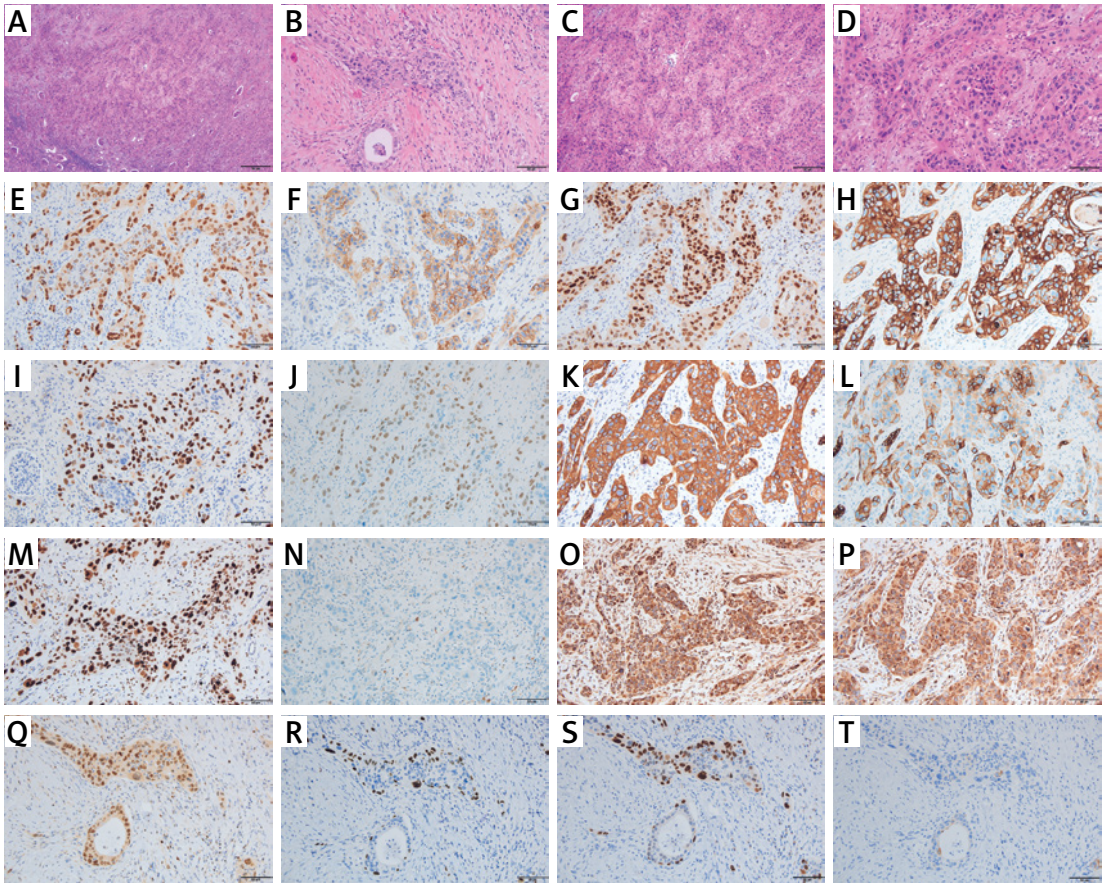

Figure 2. Histological examination and immunohistochemistry of the tumor. **A–D** – H&E staining. **E–P** – Immunohistochemistry of the tumor, 200× magnification. **Q–T** – Immunohistochemistry of the glandular differentiation area, 200× magnification. **A** – Microscopy shows infiltrative tumor growth with nested arrangements and small necrotic foci, magnification 40×. **B** – Focal glandular structures with necrotic debris within the lumina, magnification 100×. **C**, **D** – Tumor cells show indistinct borders, eosinophilic cytoplasm, marked nuclear pleomorphism, and atypical mitoses, magnification 100× for **C** and 200× for **D**. **E** – PAX8 (+). **F** – CAIX (+). **G** – GATA-3 (squamous area +). **H** – CK5/6 (+). **I** – P40 (mostly positive +). **J** – P63 (mostly positive +). **K** – CK (squamous area +). **L** – CK7 (small squamous area +). **M** – Ki-67 (Li: 70%). **N** – CD117 (-). **O** – SDHB (+). **P** – FH (+). **Q** – GATA-3 (+). **R** – P40 (-). **S** – P63 (-). **T** – CK20 (-). Immunohistochemistry, 200× magnification

morphological and immunohistochemical findings supported a final diagnosis of primary renal parenchymal squamous cell carcinoma, non-keratinizing type, with focal glandular differentiation. In this case, "non-keratinizing" describes the predominant morphology of the tumor, while its squamous nature was supported by CK5/6, P40, and P63 expression. Focal glandular differentiation referred to localized gland-forming structures within the tumor. Histological examination of the dissected left renal hilar lymph nodes showed no metastasis. However, carcinoma infiltration was identified in the perihilar perivascular adipose tissue. The pathological stage was pT3aN0.

The patient did not receive any adjuvant therapy. During the 13-month follow-up, regular clinical assessments and contrast-enhanced CT examinations showed no evidence of local recurrence or distant metastasis. However, long-term follow-up remains necessary.

To further understand the clinical characteristics and management of this rare disease, we conducted a literature review using PubMed. The search was performed up to November 2025 using the following keywords: "primary renal parenchymal squamous cell carcinoma", "renal squamous cell carcinoma", and "kidney squamous cell carcinoma". The reference lists of relevant articles were also manually screened to identify additional eligible reports. Cases were included if they were histopathologically confirmed as primary renal parenchymal SCC and provided sufficient clinicopathological information. Cases were excluded if they involved primary renal pelvic SCC, urothelial carcinoma with squamous differentiation, metastatic SCC involving the kidney, or lacked adequate pathological confirmation. Overall, 26 previously reported cases were identified and included in the literature review, as summarized in Table I. The present case was described separately and

Table I. Clinical summary of 26 previously reported cases of primary renal parenchymal squamous cell carcinoma of the kidney

No.	Author	Number of cases	Age	Presentation	Location	Treatment	Tumor extent	Renal stone	Staghorn calculus	Xanthogranulomatous pyelonephritis	Involvement of renal pelvis	Chemotherapy	Prognosis
1	Wu *et al.*	1	66	Loin pain and fever for 1 week	Left kidney	Radical nephrectomy with lymph node dissection	9.5 cm × 5.7 cm × 5.6 cm, with para-aortic lymph node metastasis (pT2aN1)	Present	NR	Present	Present	Present	Metastasis to the right lung and adrenal region at 10 months after surgery and alive at 12 months
2	Varshney *et al.*	1	66	Flank pain for 20 days	Upper pole of the left kidney	Open subcapsular nephrectomy	With renohepatic fistula (pT3N1)	Present	Present	Present	Present	NR	General well-being at 2 months and died from acute myocardial infarction 6 months after surgery
3	Priyatharsan *et al.*	1	72	Left lower abdominal pain, intermittent fever, loss of appetite and weight for over 1 month	Lower pole of the left kidney	Palliative radiotherapy	pT3Nx	Present	Present	NR	Present	NR	NR
4	Kasahara *et al.*	1	70	Fatigue, low fever and pyuria	Left kidney	Open nephrectomy	pT3Nx	Present	Present	Present	Present	NR	Died at 2 months after surgery
5	Hosseinzadeh *et al.*	1	51	Flank pain and hematuria	Right kidney	Radical nephrectomy	Invading to the perinephric fat (pT3aNx)	Present	Present	NR	Present	NR	Metastasis to liver at 6 months after primary surgery and died at 1 year after pathologic diagnosis

Table I. Cont.

No.	Author	Number of cases	Age	Presentation	Location	Treatment	Tumor extent	Renal stone	Staghorn calculus	Xanthogranulomatous pyelonephritis	Involvement of renal pelvis	Chemotherapy	Prognosis
6	Takanashi *et al.*	1	73	Renal mass on ultrasonography	Upper pole of the right kidney	Radical nephrectomy with partial hepatectomy	9.0 × 9.0 cm, with adrenal and hepatic invasion (pT4)	Present	NR	NR	Present	NR	Retroperitoneal recurrence and multiple lung metastases appeared 2 months after surgery, then death
7	Oh and Kim	1	61	Flank pain and weight loss for 2 months	Lower pole of the right kidney	Radical nephrectomy with right hemicolectomy	9.0 × 8.0 cm, with ascending colon invasion (pT4N0)	Present	NR	NR	NR	NR	Alive and disease free at 5 months after surgery
8	Yu *et al.*	1	64	Left lower back pain with intermittent fever	Left kidney	Radical resection of the left renal tumor with colon repair	Infiltrated the pancreatic body and tail and the spleen, with retroperitoneal lymph node metastasis (cT4N2)	NR	NR	Present	NR	Present	Alive and disease free at 9 months after surgery
9	Junejo *et al.*	1	67	Gross hematuria associated with clots	Right kidney	Radical nephrectomy	pT4Nx	NR	NR	NR	NR	NR	Alive and disease free during the last visit to the urology clinic
10	Junejo *et al.*	1	50	Flank pain for 4 months	Right kidney	Radical nephrectomy, excision of nephrocutaneous fistula tract and right hemicolectomy en bloc resection	pT4N0	NR	NR	NR	NR	NR	NR

Table I. Cont.

No.	Author	Number of cases	Age	Presentation	Location	Treatment	Tumor extent	Renal stone	Staghorn calculus	Xanthogranulomatous pyelonephritis	Involvement of renal pelvis	Chemotherapy	Prognosis
11	Junejo *et al.*	1	45	Flank pain and dysuria for 1 month	Left kidney	Radical nephrectomy	pT4N1	NR	NR	NR	NR	Present	Metastasis to the left renal fossa, mediastinal lymph nodes, and multiple pulmonary nodules and died at 1 year after diagnosis
12	Terada	1	73	Hematuria and lumbago	Multiple: bladder, left ureter, and left kidney	Cystectomy and nephroureterectomy	Entire kidney parenchyma	NR	NR	NR	NR	NR	Alive and disease free at 3 months after surgery
13	Shah *et al.*	1	48	Abdominal pain and dysuria for 2 months	Right kidney	Radical nephrectomy	pT3Nx	Present	Present	NR	NR	NR	Alive and disease free at 6 months after surgery
14	Kulshreshtha	1	60	Weight loss for 3 months	Mid and lower pole of the left kidney	Radical nephrectomy with lymph node dissection	6.5 cm × 5.5 cm, with Gerota's fascia invasion and para-aortic lymph node metastasis (pT4N1)	NR	NR	NR	NR	NR	Alive and disease free at 13 months after surgery
15	Zheng *et al.*	1	51	Hematuria and lumbago for 2 weeks	Right kidney	Radical nephrectomy with lymph node dissection	6.0 cm × 6.0 cm, with perirenal fat invasion and para-aortic lymph node metastasis (pT3aN1)	Present	NR	NR	NR	NR	Metastasis to the liver and inferior vena cava at 4 months, and died at 6 months after surgery

Table I. Cont.

No.	Author	Number of cases	Age	Presentation	Location	Treatment	Tumor extent	Renal stone	Staghorn calculus	Xanthogranulomatous pyelonephritis	Involvement of renal pelvis	Chemotherapy	Prognosis
16	Liang *et al.*	1	52	Renal cyst found in physical examination	Upper pole of the right kidney	Robot-assisted partial nephrectomy	8.3 cm × 8.2 cm × 8.1 cm (pT2aNxM0)	NR	NR	NR	NR	NR	Alive and disease free at 6 months after surgery
17	Fotovat *et al.*	1	41	Flank pain and dysuria for 3 months	Lower pole of the left kidney	Radical nephrectomy	Perirenal fat invasion and para-aortic lymph node metastasis (pT3aN1)	Present	NR	Present	NR	Present	Metastasis to the ovary at 8 months after surgery
18	Wang *et al.*	1	61	Hematuria and lumbago for 2 months	Right kidney	Radical nephrectomy	Perirenal fat invasion (pT3aNx)	NR	NR	Present	NR	NR	Alive and disease free at 1 month after surgery
19	Zhang *et al.*	1	61	Intermittent flank pain for 2 months	Lower pole of the right kidney	Radical nephrectomy	With perirenal fat invasion (pT3aNx)	NR	NR	NR	NR	NR	Alive and disease free at 3 months after surgery
20	Chang *et al.*	1	69	Flank pain and right lower limb swelling for several days	Right kidney	Right nephrectomy	pT3aNx	Present	Present	Present	NR	NR	Alive and disease free at 4 months after surgery
21	Veerabathini *et al.*	1	54	Fatigue, vomiting and significant weight loss for 1 month	Right kidney	Comfort measures only	pT3aN1	Present	Present	Present	NR	NR	Decompensated complications of the carcinoma and died before surgery

Table I. Cont.

No.	Author	Number of cases	Age	Presentation	Location	Treatment	Tumor extent	Renal stone	Staghorn calculus	Xanthogranulomatous pyelonephritis	Involvement of renal pelvis	Chemotherapy	Prognosis
22	Sahoo *et al.*	1	50	Right abdomen pain for 6 months	Upper pole of the right kidney	Radical nephrectomy	8.0 cm × 6.0 cm (pT2aNx)	NR	NR	NR	NR	NR	Alive and disease free at 6 months after surgery
23	Ghosh and Saha	1	51	Dull and intermittent flank pain for 5 months	Lower pole of the right kidney	Radical nephrectomy	5.8 cm × 5.5 cm (pT1bN0)	NR	NR	NR	NR	NR	Alive and disease free at 12 months after surgery
24	Liu *et al.*	1	54	Flank pain and abdominal mass for 6 months	Upper pole of the left kidney	Radical nephrectomy	pT3aN1	Present	NR	NR	NR	Present	Metastasis to adrenal, lymph, and uterine appendage and died 7 months after surgery
25	Jia *et al.*	1	42	Flank pain for more than 20 days	Lower pole of the right kidney	Radical nephrectomy	pT3N1	Present	NR	NR	NR	NR	NR
26	Sun *et al.*	1	69	Left lumbago	Left kidney	NR	pT3N1	Present	NR	NR	NR	NR	NR
Total		26											

Note: This table summarizes 26 previously reported cases of primary renal parenchymal squamous cell carcinoma described in 24 published articles. The present case was not included in this literature-based summary. NR – not reported.

was not included in the literature-based statistical summary.

Among the 26 previously reported cases, renal calculi were explicitly documented in 15 patients. In the present case, renal calculi and xanthogranulomatous pyelonephritis (XGP) were clinically and pathologically absent, whereas focal involvement of the renal pelvic urothelium was identified. This combination is noteworthy and suggests that renal pelvic urothelial involvement may occur in primary renal parenchymal SCC even in the absence of chronic calculous disease or XGP. Notably, from a diagnostic perspective, our patient presented with left flank pain as the only symptom, without typical urinary manifestations such as hematuria, urinary frequency, urgency, or dysuria. However, the literature review indicates that flank or abdominal pain is the most common clinical symptom of primary renal parenchymal SCC [2, 3], whereas genitourinary symptoms were observed in fewer than half of the documented cases [2, 4–9].

Renal pelvic urothelial involvement has been reported in only a small number of published cases of primary renal parenchymal SCC [1, 4, 10–13]. Primary renal parenchymal SCC tends to invade the perirenal adipose tissue and adjacent organs, including the colon, liver, spleen, and pancreas, and fistula formation has also been reported [5, 10, 13–15]. SCC is generally characterized by marked local invasiveness and regional spread, whereas urothelial carcinoma may show a greater tendency toward distant metastasis [16]. Due to the lack of specific early urinary symptoms, primary renal parenchymal SCC is frequently diagnosed at an advanced stage, leading to a poor prognosis [4, 5, 7, 12, 17, 18].

Herein, the imaging findings closely correlated with the histopathological findings. On CT and MRI scans, the heterogeneous enhancement and internal non-enhancing areas corresponded to the infiltrative growth pattern of the tumor and its small necrotic foci, respectively. Notably, the suspicious left renal vein involvement on CT and MRI was supported by pathological evidence of carcinoma infiltration in the perihilar perivascular adipose tissue. According to the eighth edition of the American Joint Committee on Cancer (AJCC) TNM staging system [19], the radiological stage was T3a, which was consistent with the pathological stage (pT3a). This imaging–pathology correlation highlights the value of multimodal imaging in assessing tumor extent and vascular involvement, while also providing findings that may correlate with underlying histopathological features, thereby aiding preoperative staging and surgical planning.

Previous reports have suggested that nephrolithiasis and hydronephrosis may be associated with the development of renal SCC [20]. However, whether stones cause this rare tumor or the tumor leads to stone formation remains unclear [21, 22]. Recent studies have suggested that renal calculi may contribute to a pro-inflammatory, pro-tumorigenic microenvironment, while molecular analyses have identified alterations in VHL, PBRM1, and MET [23]. These findings suggest a possible link between chronic irritation and renal tumorigenesis, although the underlying mechanisms remain unclear. The literature review revealed that 69% of patients with XGP had renal/ureteral stones and 48% of patients had staghorn calculi. Nephrolithiasis is a hallmark of XGP and often requires exclusion of primary renal parenchymal SCC [8]. XGP has been reported in several previously published cases of primary renal parenchymal SCC, suggesting a possible association between chronic inflammatory renal disease and tumor development [1, 3, 8–10, 12, 15, 17].

Radical nephrectomy remains the mainstay of treatment for localized primary renal parenchymal SCC [21, 24]. The literature review showed that only five patients received postoperative chemotherapy. Among these patients, four developed metastases, involving sites such as the adrenal gland, perirenal lymph nodes, uterine adnexa, mediastinum, and lung, and one patient died due to chemotherapy-related complications [8]. Yu *et al.* reported one patient who remained alive without recurrence or metastasis 9 months after surgery and postoperative chemotherapy [15]. However, this isolated observation with a short follow-up period does not establish the efficacy of chemotherapy. Therefore, the efficacy and safety of chemotherapy for primary renal parenchymal SCC remain unclear, and further evidence from additional cases with longer follow-up is needed. EGFR-targeted therapies have shown clinical activity in several epithelial malignancies, including non-small cell lung cancer, colorectal cancer, and head and neck SCC [25, 26]. Favorable outcomes have also been reported in selected cases of upper tract and bladder SCC [27, 28]. However, their efficacy in primary renal parenchymal SCC remains unknown [14, 27, 29]. Given the biological similarities among SCCs, investigating EGFR expression and mutation patterns in primary renal parenchymal SCC may help identify patients who could benefit from this targeted approach.

A notable limitation of this case report is the relatively short follow-up period, which precludes firm conclusions about prognosis. In addition, the literature review was narrative rather than systematic, and the available evidence was limited by the small number of reported cases, heterogeneous clinical data, and incomplete reporting in some previous publications. This case highlights

the diagnostic challenges of primary renal parenchymal SCC. Even in the absence of typical symptoms or risk factors such as renal calculi or XGP, primary renal parenchymal SCC may show focal renal pelvic urothelial involvement, which should be distinguished from primary renal pelvic SCC or urothelial carcinoma with squamous differentiation. Radical nephrectomy remains the mainstay of treatment, while the role of adjuvant therapy requires further investigation. Further follow-up and additional case data are needed to clarify optimal management and long-term outcomes.

Acknowledgments

Lingze Hu, Dilare Aximu and Qianqian Yang contributed equally to this work and should be designated as co-first authors.

Funding

This work was supported by the National Natural Science Foundation of China (82303499) and the Research Project of Hubei Preventive Medicine Association (2025SWGKY079). The technical assistance of Mrs. Lan Yang is gratefully acknowledged.

Ethical approval

Written informed consent was obtained from the patient for publication of the details of their medical case and any accompanying images. The Ethics Committee of Zhongnan Hospital of Wuhan University approved this study (approval number 2020102). We certify that this study was conducted in compliance with ethical standards, including the Declaration of Helsinki.

Conflict of interest

The authors declare no conflict of interest.

References

1. Wu J, Wang L, Zhao P, Lin F, Xu Z. Primary renal parenchymal squamous cell carcinoma involving the renal pelvis: a case report and review of the literature. Urol Case Rep 2025; 61: 103083.
2. Shah HA, Khan AA, Hussain SM, Ali MA. Squamous cell carcinoma; a rare complication of long-standing renal stones: case report and an overview. J Pak Med Assoc 2025; 75: 492-4.
3. Chang TH, Tseng JS. Rare squamous cell carcinoma of the kidney with concurrent xanthogranulomatous pyelonephritis: a case report and review of the literature. Open Med 2021; 16: 128-33.
4. Hosseinzadeh M, Mohammadzadeh S. Primary pure squamous cell carcinoma of kidney associated with multiple stag horn stones. Int Med Case Rep J 2020; 13: 261-3.
5. Junejo NN, Kamal MH, Aquil S, Al Rahbi F, Al Badaai GAR, Siddiqui KM. Primary squamous cell carcinoma of the kidney: a case series. Oman Med J 2025; 40: e721.
6. Terada T. Synchronous squamous cell carcinoma of the kidney, squamous cell carcinoma of the ureter, and sarcomatoid carcinoma of the urinary bladder: a case report. Pathol Res Pract 2010; 206: 379-83.
7. Zheng ZH, Shao B, Xu CM, et al. Primary parenchymal squamous cell carcinoma of the kidney: a case report. World J Clin Cases 2025; 13: 100037.
8. Fotovat A, Gheitasvand M, Amini E, Ayati M, Nowroozi MR, Sharifi L. Primary squamous cell carcinoma of renal parenchyma: case report and review of literature. Urol Case Rep 2021; 37: 101627.
9. Wang Z, Yan B, Wei YB, et al. Primary kidney parenchyma squamous cell carcinoma mimicking xanthogranulomatous pyelonephritis: a case report. Oncol Lett 2016; 11: 2179-81.
10. Varshney B, Nalwa A, Yadav T, Choudhary G. Renal squamous cell carcinoma presenting with renohepatic fistula: a rare amalgam. Ochsner J 2023; 23: 72-6.
11. Priyatharsan K, Balagobi B, Heerthikan K, Thulasi T, Priyanka A, Sureska G. A rare case of renal squamous cell carcinoma presenting with psoas sign. Int J Surg Case Rep. 2023; 110: 108732.
12. Kasahara R, Kawahara T, Tajiri R, Uemura H, Kitami K. Renal squamous cell carcinoma with Staghorn calculus. Case Rep Oncol 2020; 13: 403-7.
13. Takanashi M, Asaoka M, Imano M, et al. Primary squamous cell carcinoma of the kidney with hepatic invasion. IJU Case Rep 2024; 7: 408-13.
14. Oh CK, Kim JY. Primary squamous cell carcinoma of the kidney parenchyma with ascending colon invasion: a case report and literature review. Int J Surg Case Rep 2022; 91: 106762.
15. Yu H, Yu L, Li J, et al. A case report of complete pathological remission after chemotherapy in a patient with primary renal squamous cell carcinoma. Transl Androl Urol 2021; 10: 997-1005.
16. Martin JW, Carballido EM, Ahmed A, et al. Squamous cell carcinoma of the urinary bladder: systematic review of clinical characteristics and therapeutic approaches. Arab J Urol 2016; 14: 183-91.
17. Veerabathini BC, Manthani K, Gandhi S, Duddala N. A very rare case of primary renal squamous cell carcinoma presenting with xanthogranulomatous pyelonephritis on radiological imaging. Cureus 2020; 12: e11871.
18. Liu XH, Zou QM, Cao JD, Wang ZC. Primary squamous cell carcinoma with sarcomatoid differentiation of the kidney associated with ureteral stone obstruction: a case report. World J Clin Cases 2022; 10: 11942-8.
19. Elkassem AA, Allen BC, Sharbidre KG, Rais-Bahrami S, Smith AD. Update on the role of imaging in clinical staging and restaging of renal cell carcinoma based on the AJCC 8th Edition, From the AJR Special Series on Cancer Staging. AJR Am J Roentgenol 2021; 217: 541-55.
20. Bandyopadhyay R, Biswas S, Nag D, Ghosh AK. Squamous cell carcinoma of the renal pelvis presenting as hydronephrosis. J Cancer Res Ther 2010; 6: 537-9.
21. Zhang X, Zhang Y, Ge C, Zhang J, Liang P. Squamous cell carcinoma of the renal parenchyma presenting as hydronephrosis: a case report and review of the recent literature. BMC Urol 2020; 20: 107.
22. Kalayci OT, Bozdag Z, Sonmezgoz F, Sahin N. Squamous cell carcinoma of the renal pelvis associated with kidney stones: radiologic imaging features with gross and histopathological correlation. J Clin Imaging Sci 2013; 3: 14.
23. Li J, Zhao C. Investigating the co-occurrence of urinary calculi and renal carcinoma: a comprehensive analysis

of clinical and molecular associations. Arch Med Sci 2025; DOI: https://doi.org/10.5114/aoms/210333.
24. Sun W, Zhang L, Shao L, Wang J. An unusual case of primary renal squamous cell carcinoma with bone metastasis. Asian J Surg 2023; 46: 1515-6.
25. Vaquero J, Pavy A, Gonzalez-Sanchez E, Meredith M, Arbelaiz A, Fouassier L. Genetic alterations shaping tumor response to anti-EGFR therapies. Drug Resist Updat 2022; 64: 100863.
26. Brzozowska M, Wierzba W, Szafraniec-Buryło S, et al. Overall survival of patients with EGFR mutation-positive non-small-cell lung cancer treated with erlotinib, gefitinib or afatinib under drug programmes in Poland – real-world data. Arch Med Sci 2021; 17: 1618-27.
27. Wucherpfennig S, Rose M, Maurer A, et al. Evaluation of therapeutic targets in histological subtypes of bladder cancer. Int J Mol Sci 2021; 22: 11547.
28. Deuker M, Stolzenbach LF, Collà Ruvolo C, et al. Upper urinary tract tumors: variant histology versus urothelial carcinoma. Clin Genitourin Cancer 2021; 19: 117-24.
29. Sahoo TK, Das SK, Mishra C, et al. Squamous cell carcinoma of kidney and its prognosis: a case report and review of the literature. Case Rep Urol 2015; 2015: 469327.